
Author Query Form

Journal Title: Journal of Engineering Tribology, Proceedings of the Institution of Mechanical Engineers Part J [PIJ]

Article Number: 503151





Dear Author/Editor,

Greetings, and thank you for publishing with SAGE. Your article has been copyedited and typeset, and if we have any queries for you they are listed below. Please address these queries when you return your proof corrections. Thank you for your time and effort.

Please ensure that you have obtained and enclosed all necessary permissions for the reproduction of artistic works, (e.g. illustrations, photographs, charts, maps, other visual material, etc.) not owned by yourself, and ensure that the Contribution contains no unlawful statements and does not infringe any rights of others, and agree to indemnify the Publisher, SAGE Publications Ltd, against any claims in respect of the above warranties and that you agree that the Conditions of Publication form part of the Publishing Agreement.

Any colour figures have been incorporated for the on-line version only. Colour printing in the journal must be arranged with the Production Editor, please refer to the figure colour policy outlined in the e-mail.

Please assist us by clarifying the following queries:

1.  Please clarify whether the '^' symbols given in equations are correct.
2. Please cite figure citations in sequential order. 
3. Please provide the date of the proceedings, place, publisher-location details and page range. 
4. Kindly check that two R's are given. 

A numerical procedure for the wheel profile optimisation on railway vehicles

Mirko Ignesti, Alice Innocenti, Lorenzo Marini, Enrico Meli and Andrea Rindi

Proc IMechE Part J:
J Engineering Tribology
0(0) 1–17
© IMechE 2013
Reprints and permissions:
sagepub.co.uk/journalsPermissions.nav
DOI: 10.1177/1350650113503151
pij.sagepub.com



Abstract

The reduction of wear due to wheel–rail interaction is a fundamental aspect in the railway field, mainly correlated to safety, maintenance interventions and costs. In this work, the authors present an innovative wheel profile optimisation procedure, specifically designed with the aim of improving the wear and stability behaviour of the standard ORE S1002 wheel profile matched with the UIC60 rail profile canted at $1/20$ rad, which represents the wheel–rail combination adopted in Italian railway line; this matching shows poor wear performance due to the non-conformal contact. A new wheel profile, conventionally named DR2, has been developed by the authors in collaboration with Trenitalia S.p.A. The DR2 wheel profile is designed to guarantee the same kinematic characteristics of the matching formed by ORE S1002 wheel profile and UIC60 rail profile with inclination angle α_p equal to $1/40$ rad, widely common in European railways and characterised by good performances in both wear and kinematic behaviour. The evolution of wheel profiles due to wear has been evaluated through a wear model developed and validated by the authors in previous works. In the present research the investigated trainset is the passenger vehicle ALSTOM ALn 501 “Minuetto”, which is usually equipped with wheelsets having the standard ORE S1002 wheel profile in Italian railways. The entire model has been simulated on a virtual track specifically developed to represent a statistical description of the whole Italian line; the innovative statistical approach has been employed to obtain accurate results in reasonable computational times. The data necessary to build the virtual track and the vehicle model were provided by Trenitalia S.p.A. and Rete Ferroviaria Italiana (RFI).

Keywords

Multibody modeling of railway vehicles, wheel–rail contact, wheel–rail wear modeling, wheel–rail profile optimisation

Date received: 12 February 2013; accepted: 1 August 2013

Introduction

Wear phenomena due to wheel–rail interaction represent a critical aspect in railway applications; in fact, the consequent evolution of rail and wheel profiles involves serious effects on dynamical characteristics of vehicles. Profile changes lead also to higher maintenance cost, mainly concerned with the periodically re-profiling operations of wheels and the undesirable replacements of rails.

The shape optimisation of profiles for the reduction of wear at the wheel–rail interface represents an important aspect in railway field and various approaches were developed to obtain a satisfactory combination of wheel and rail profiles.^{1–4} The optimum matching is usually pursued through the design of a new wheel profile which matches an existing rail profile, because the cost of rail interventions is notably higher compared with the cost of turning or replacement of the wheels.

This paper describes the design/optimisation procedure and the behaviour in wear reduction of an innovative wheel profile, named DR2 wheel profile,⁵

developed by the authors in collaboration with Trenitalia and RFI, with the aim of reducing wheel–rail wear that occurs when coupling the European standard wheel profile ORE S 1002⁶ and UIC60/E1⁷ rail profile with inclination angle α_p equal to $1/20$ rad, adopted in Italian line; this combination is characterized by poor wear performance due to the initial non-conformal contact condition. The design/optimisation procedure of DR2 wheel profile aims to maintain, with the new profile, the kinematic characteristics of the matching formed by ORE S1002 wheel profile and UIC60 rail profile with inclination angle α_p equal to $1/40$ rad. Such matching is commonly adopted in European railways and showed low wear level, due to

Department of Energy Engineering, University of Florence, Firenze, Italy

Corresponding author:

Enrico Meli, Department of Energy Engineering, University of Florence, via di S. Marta 3, Florence 50100, Italy.
Email: enrico.meli@unifi.it

the fact that it was developed from studies based on partly worn wheels, characterized by a shape remained steady for a long time. On the contrary, the matching ORE S1002-UIC60 canted at 1/40 rad is not only characterized by good kinematic performances but it also shows a high equivalent conicity value, leading to instability problems. The matching ORE S1002-UIC60 with a cant of 1/20 rad exhibits a wider contact area at the outer parts of the wheel tread, involving lower equivalent conicity values and consequent improvement in stability characteristics. The disadvantage consists in poor wear performances.

The proposed wheel optimisation procedure is based on the wheelset and the track parameters, not only on the parameters of a single pair wheel/wheelset. In the present research activity rail gauge and wheelset gauge are assumed to be constant.

The trainset to be investigated in order to evaluate the capability in wear reduction of the innovative profile is the passenger vehicle ALSTOM ALn 501 "Minuetto", which is equipped with wheelsets having the standard ORE S1002 wheel profile and matched with the UIC60 rail profile canted at 1/20 rad in Italian railway. This particular vehicle exhibited a poor wear performance, as verified for example by experimental measurements performed on the Aosta Pre-Saint Didier line.^{8,9} In this research the wheel profile optimisation procedure has been tested on the entire Italian line on which the Minuetto operates; an improvement in the validation will be reached testing the algorithms on other vehicles (also less critical in terms of wear than the Minuetto) and by means of future experimental tests, which are already planned by Trenitalia.

The evolution of wheel profiles has been evaluated by means of a model specifically developed for the wear assessment, which has been validated by the authors in previous works^{8,9} in collaboration with Trenitalia S.p.A. and Rete Ferroviaria Italiana (RFI), which provided the experimental data relating to some tests performed with the vehicle to be investigated on the Aosta-Pre Saint Didier line.⁵ This rail road section turned out to be quite critical in terms of wear for its sharpness and for the characteristics of the "Minuetto", when operated on that railway track.^{10,11}

The general architecture of the developed wear model comprises two mutually interactive parts: the vehicle model (multibody model and wheel and rail 3D global contact model) and the wear model (local contact model, wear estimation and profiles updating).¹²

The multibody model of the vehicle is implemented in the Simpack Rail environment and it takes into account all the significant degrees of freedom of the vehicle. The 3D global contact model, developed by the authors in previous works,^{13,14} detects the wheel-rail contact points by means of an innovative algorithm based on suitable semi-analytical procedures

and then, for each contact point, calculates the contact forces by means of Hertz's and Kalker's theory.¹⁵⁻¹⁷ Thanks to the numerical efficiency of the new contact model, it can interact directly online with the multibody model during the dynamic simulation of the vehicle, without look-up table (LUT) with saved pre-calculated values of contact parameters. Wear evolution is performed by means of a model based on a local contact model (in this case the Kalker's FASTSIM algorithm^{15,16}) and on an experimental relationship for the calculation of the worn material available in literature^{12,18-20} (based on the work of the frictional forces). The wear model, starting from the outputs of the vehicle model (contact points, contact forces and global creepages), is able to calculate the total amount of removed material due to wear in dry conditions and its corresponding distribution along the wheel profile. Since the aim of the present research activity consists in the optimisation of wheel profile, only wheel wear is considered and the evolution of a single mean wheel profile for the whole vehicle is studied. The removal process of the material takes into account the three-dimensional structure of the contact bodies since the initial distribution of worn material (and the following averages) has been evaluated along all the geometric dimensions of the 3D bodies.

In the present work the authors present an innovative statistical approach to perform wear analysis on complex railway track in reasonable computational time for practical purpose and accurate results, representing an innovative aspect in wheel wear research field. Therefore, all the simulations are performed on a virtual track, specifically designed to represent a statistical representative description of the whole Italian railway line travelled by the ALn 501 Minuetto.⁵ This statistical railway line is a set of N_c curvilinear track (plus the straight track) characterized, as it will be explained in the following sections, by a specific radius R , superelevation h , velocity V and statistical weights p_k , representing the occurrence frequency of each curvilinear track with respect to the entire investigated line (with $1 \leq k \leq N_c$). A mean constant and statically representative worn rail profile is then associated to each curvilinear track of the statistical railway line⁵ to perform the simulations on a worn rail profile (instead of a new one, which is unrepresentative) that most frequently is present in that class of curve. At this phase of the research, track irregularities have not been considered. Suitable irregularities associated to each curve class will be chosen in the next phases thanks to new experimental data provided from Trenitalia S.p.A.

General architecture of the model

The general architecture of the model consists of a discrete procedure separated into two parts that work alternatively at each procedure step: the *vehicle*

model and the wear model. The general layout of the entire model is illustrated in Figure 1. The *vehicle model*, modelled in the commercial Multibody Software Simpack, is the part responsible for the dynamical simulations and it is based on the online mutual interaction of the multibody model of the vehicle to be investigated (in this work the ALSTOM ALn 501 “Minuetto”), the characteristics of the investigated track, the relative operating conditions and the 3D wheel–rail global contact model.^{13,14} More specifically, at each integration step during time-domain dynamic simulation, the multibody model evaluates the kinematic variables (position, orientation and their derivatives) of the considered vehicle at each wheelset. These variables are then passed to the 3D global contact model, whose task consists in the calculation of the global contact parameters: contact points, contact areas, global creepages and contact forces. Once the contact problem has been solved, the values of the global forces are sent back to the multibody model and the dynamical simulation proceeds with the next time integration step.

The *wear model* is the part of the procedure concerning the computation of wheel profile evolution and it predicts the amount of worn material to be removed from the wheel surfaces. The wear model can be sub-divided into three parts: the local contact model, the evaluation of worn material and the profile updating. Firstly, the local contact model (whose

approach is based on Hertz’s local theory and Kalker’s simplified theory implemented in FASTSIM algorithm^{15,16}) estimates the local contact pressures and creepages and detects the creep zone of the contact area. Then, according to an experimental relationship between the worn material and the energy dissipated by friction forces at the contact interface,^{12,18–20} the quantity of removed material on wheel surface is computed on the creep area. This estimation is performed hypothesizing dry contact friction at the wheel–rail interface. Last step of the wear prediction procedure consists in updating the profiles: the worn profiles are derived from the original ones using an appropriate update strategy. The single mean profile (the same one for all the vehicles) is then fed back as input to the entire *vehicle model* and the whole model procedure proceeds with the next discrete step.

In the present work the total mileage to be simulated km_{tot} is subdivided into several steps characterized by a value km_{step} of the traveled distance and the wheel profiles are supposed to be constant within each discrete step. The adopted updating strategy for the km_{step} choice is a key point since it may appreciably affect the results and its main task consists in evaluating the mileage after which wheel profiles should be updated, that is the distance km_{step} simulated during each discrete step. Different updating strategies are available in literature and the most significant are: the constant step update strategy,^{21,22} which is

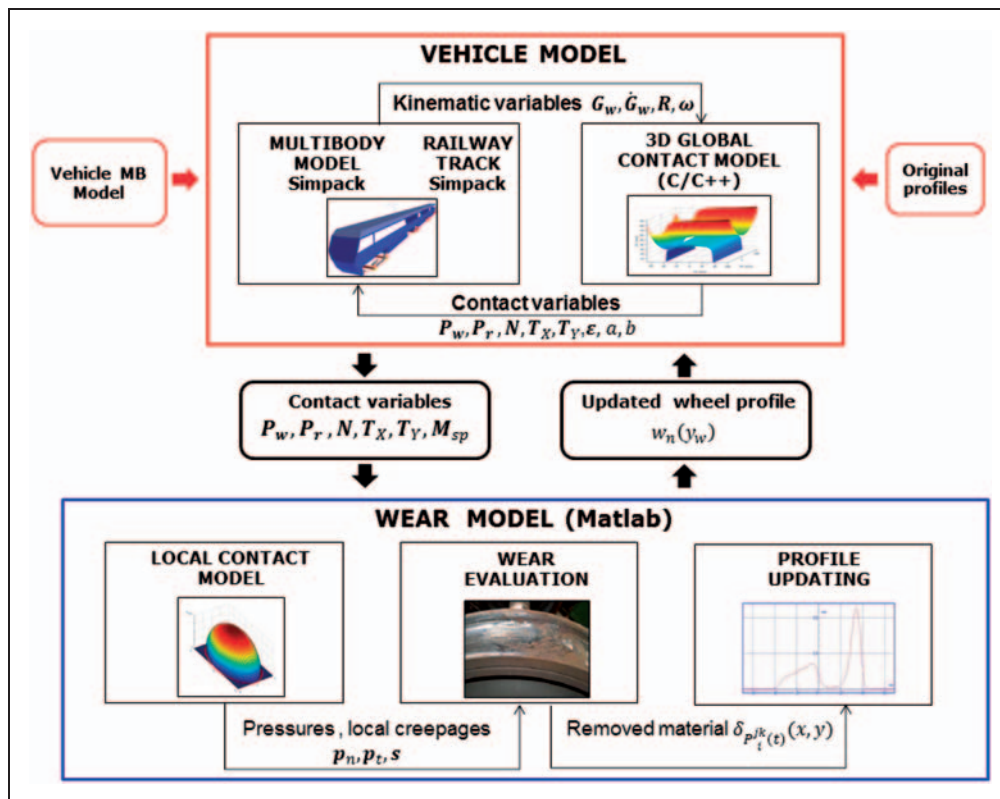


Figure 1. General architecture of the model.

characterized by a constant value km_{step} of the discrete step and the adaptive step update strategy,^{8,18,20} wherein the wheel profile is updated when a given threshold Δ_{fix} of the maximum value of cumulative wear depth is reached and the value km_{step} is consequently variable. During this research activity the adaptive step has been adopted for its capacity in representing the nonlinear behaviour of the wear evolution, particularly in the first phases when wheel–rail contact is non-conformal.

The entire *wear model* has been implemented in the Matlab environment.

The vehicle model

The present section deals with the description of the *vehicle model*. First of all, the multibody representation for the dynamical simulations of the studied vehicle is introduced. Then the algorithm that models the 3D global contact is briefly explained.

The multibody model. The trainset investigated during this research is ALSTOM ALn 501 “Minuetto”, a passenger transport unit widespread in Italian Railways, equipped with wheelsets having the standard ORE S1002 wheel profile matching with UIC60 rail profile canted at 1/20 rad. This particular vehicle exhibits in fact severe wear problems mainly caused by the wheel–rail matching. Its mechanical structure and inertial, elastic and damping properties can be found in literature.⁵ Table 1 shows the main characteristics of the considered vehicle.

The multibody model of the vehicle has been implemented in the Simpack environment (see Figure 2) and it mainly consists of car bodies connected by means of the secondary suspensions to the vehicle bogies, which in turn are linked to wheelsets through the primary suspensions. Totally, the multibody model is made up of 31 rigid bodies: three coaches, four bogies (two motor bogies at the vehicle ends and two intermediate trailer bogies interposed between two successive coaches), eight wheelsets (two for each bogie), 16 axleboxes (two for each wheelset).

Table 1. Main characteristics of the ALn 501 Minuetto DMU.

Length	51.9 m
Width	2.95 m
Height	3.82 m
Bogie pivot distances	14.8-13.8-14.8 m
Bogie wheelbase	2.80 m
Unladen weight	100 t
Wheel arrangement	Bo-2-2-Bo
Wheel diameter	850 mm
Max speed	130 km/h

Wheel–rail interaction and suspensions modeling are key points in railway vehicle dynamics because they are strictly related to the function of support and guidance of the rail vehicle. As wear of the profiles increases, the shape of the wheel profile changes inducing performance variations in the wheelset–rail coupling and especially in the guidance of the vehicle. Wheelset guidance is strictly related to the equivalent conicity of the flange and to flange wear: high flange wear may compromise wheelset guidance capability with a consequent increase of the derailment risk (like tread wear involves hunting problems).

Suspensive system of the Minuetto (that has been designed for higher speed than the one allowed on the Aosta line and for less sharp lines) has a negative influence on wear of the wheelsets on the Aosta track because it is too rigid and causes high angles of attack and excessive guidance effect.

The dual-stage suspensions have been modelled by means of three-dimensional linear and non linear visco-elastic force elements. In the primary suspension stage the elastic elements are Flexicoil springs (constituted by two coaxial helical compression springs), while damping of the vertical relative displacement is provided by means of two non linear hydraulic dampers. The secondary stage is formed by pneumatic suspensions and it comprises the following elements: two air springs, six nonlinear dampers (lateral, vertical and anti-yaw dampers), one nonlinear traction rod, the roll bar, two nonlinear lateral bumpstops.

3D global contact model. In this research activity, a specifically developed 3D global contact model has been employed in order to improve reliability and accuracy of the contact points detection, compared to those given by the Simpack Rail contact model. The main features of the innovative adopted algorithm are the following:^{8,13,14,23}

- It is a fully 3D model that takes into account the six relative degrees of freedom (DOF) between wheel and rail; as a consequence also the attack angle is taken into account.
- It is able to support generic railway tracks and generic wheel and rail profiles.

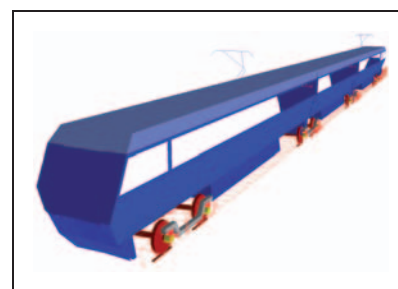


Figure 2. Global view of the multibody model of the vehicle.

- It assures a general and accurate treatment of the multiple contact without introducing simplifying assumptions on the problem geometry and kinematics and limits on the number of detected contact points.
- It assures highly numerical efficiency making possible the online implementation within the commercial multibody software (Simpack – Rail, Adams – Rail) without look-up table; in this way also the numerical performances of the commercial multibody software are improved.

As shown in Figure 1, the global contact model inputs are the kinematic variables evaluated by the multi-body model, i.e. the position, the orientation matrix R_w^r , the absolute velocity $\mathbf{O}r$ and the absolute angular velocity ω_w^r of the wheelset. Starting from these inputs, the global contact model previously developed by the authors evaluates the following outputs: positions \mathbf{P}_w^r and \mathbf{P}_r^r of the contact points, the normal \mathbf{N}^r and tangential \mathbf{T}_x^r and \mathbf{T}_y^r contact forces (Figure 3) and the spin moment \mathbf{M}_{sp}^r , the global creepages ε . Referring to the reference systems $O_r x_r y_r z_r$ and $O_w x_w y_w z_w$ shown in Figure 3, the profiles generating the wheel and rail surfaces are denoted respectively as $w(y_w)$ and $r(y_r)$. In particular, the adopted contact model is based on a two-step procedure; at the first step the contact points number and positions are determined through an innovative algorithm designed and validated by the authors.^{8,13,14} During the second step, for each detected contact point, the global contact forces (Figure 3) are evaluated using Hertz's and Kalker's global theories.¹⁵⁻¹⁷ According to Hertz's theory, the contact patch is assumed to be elliptical and characterized by semi-axes lengths dimension equal to a and b .

The contact point detection algorithm developed by the authors is based on the analytical reduction of the algebraic contact problem dimension (from a 4D problem to a simply 1D scalar problem) by means

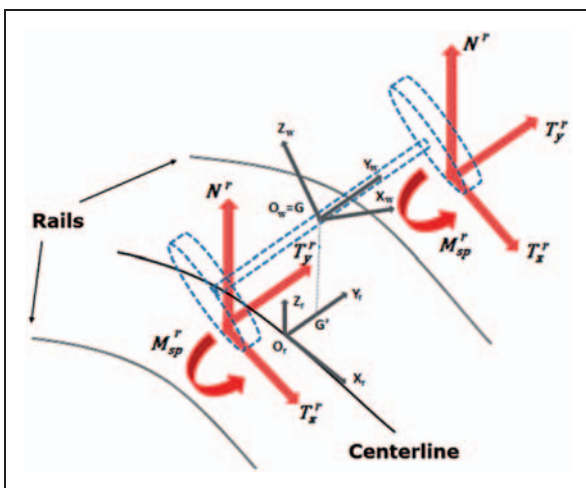


Figure 3. Global forces acting at wheel and rail interface.

of exact analytical procedures, that leads to an increase in accuracy and numerical efficiency of the contact model. More specifically wheel–rail contact formulation that has been employed in the present research activity is called *distance method* and it starts from the multi-dimensional formulation of the contact problem and reduces it to a simple mono-dimensional scalar problem. The distance method is derived starting from the two following vectorial equations (which represent a common formulation of the contact problem in multibody applications):

$$\mathbf{n}_r^r(\mathbf{P}_r^r) \wedge \mathbf{n}_w^w(\mathbf{P}_w^r) = \mathbf{n}_r^r(\mathbf{P}_r^r) \wedge R_w^r \mathbf{n}_w^w(\mathbf{P}_w^r) = \mathbf{0} \quad (1a)$$

$$\mathbf{n}_r^r(\mathbf{P}_r^r) \wedge \mathbf{d}^r = \mathbf{0} \quad (1b)$$

representing respectively the parallelism condition between the outgoing normal unit vector $\mathbf{n}_w^w(\mathbf{P}_w^r)$ to the wheel surface and the outgoing normal unit vector to the rail surface $\mathbf{n}_r^r(\mathbf{P}_r^r)$ and the parallelism between the outgoing unit vector of the rail surface and the distance vector $\mathbf{d}^r = \mathbf{P}_r^r - \mathbf{P}_w^r$, which indicates the distance between two generic points on the wheel surface and on the rail surface (where apices w and r respectively refer to wheel and rail reference systems that will be presented in section “Description of the proposed wheel profile and of the optimisation procedure”).

The system (1) results in six nonlinear equations in the four unknowns, but only four of these equations are independent; hence, the problem dimension is reduced to 4D. By means of an exact analytical procedure it is possible to express three of these variables as a function of the remaining one, with a consequent reduction of the original 4D problem to a simple 1D scalar equation.

The wear model

The inputs of the wear model are the global contact parameters estimated by the vehicle model. Since a local wear computation is required, the global contact parameters need to be post-processed and this can be achieved with the simplified Kalker's theory implemented in the FASTSIM algorithm.^{15,16} This theory starts from the global creepages (ε), the normal and tangential global forces (\mathbf{N}^r , \mathbf{T}_x^r , \mathbf{T}_y^r), the contact patch dimensions (a, b) and the material properties to compute the local distribution of normal p_n and tangential \mathbf{p}_t stresses and local slips \mathbf{s} across the wheel–rail contact area. For a more detailed description of the FASTSIM algorithm one can refer to the literature.²⁴

The distribution of worn material on wheel profile due to wear (assuming dry contact conditions) is evaluated by means of a wear experimental function, based on a law that relates the energy dissipated in the wheel–rail contact patch with the amount of worn material.^{18,19} The adopted wear function uses local

contact normal p_n and tangential \mathbf{p}_t stresses, local slips \mathbf{s} and the vehicle velocity V as the input to directly compute the specific volume of worn material $\delta_{P_{wi}^{jk}(t)}(x, y)$ ($\text{mm}^3/\text{m mm}^2$), where x and y indicate the coordinates of a generic point of the contact patch) related to the i -th contact point $P_{wi}^{jk}(t)$ on the j -th wheel relative to the k -th dynamical simulation, for unit of distance traveled by the vehicle (expressed in m) and for unit of surface (expressed in mm^2). More specifically, local contact stresses and creepages are used to evaluate the wear index I_W (expressed in N/mm^2), which represents the frictional power developed by the tangential contact pressures:

$$I_W = \frac{\mathbf{p}_t \cdot \mathbf{s}}{V}. \quad (2)$$

This index can be correlated with the wear rate K_W which represents the mass of removed material (expressed in $\mu\text{g}/(\text{m mm}^2)$) for unit of distance travelled by the vehicle and for unit of surface. The correlation chosen for the development of the present wear model is based on real data available in literature,¹⁸ which have been acquired from experimental wear tests carried out in the case of metal to metal contact with dry surfaces using a twin disc test arrangement. The experimental relationship between K_W and I_W is able to represent three wear regimes: mild, intermediate and severe wear according to the following equation:

$$K_W(I_W) = \begin{cases} 5.3 * I_W & I_W < 10.4 \\ 55.12 & 10.4 \leq I_W \leq 77.2 \\ 61.9 * I_W - 4778.68 & I_W > 77.2. \end{cases} \quad (3)$$

Once the wear rate $K_W(I_W)$ has been computed, the corresponding specific volume of worn material (for unit of distance travelled by the vehicle and for unit of surface) can be calculated as follows (expressed in $\text{mm}^3/(\text{m mm}^2)$):

$$\delta_{P_{wi}^{jk}(t)}(x, y) = K_W(I_W) \frac{1}{\rho} \quad (4)$$

where ρ represents the material density (expressed in kg/m^3).

After obtaining the amount of worn material, wheel profile needs to be updated and then it can be used as the input of the next dynamic simulation. The new profile, denoted by $w_n(y_w)$, is computed from the old one $w_o(y_w)$ and from all the calculated distributions $\delta_{P_{wi}^{jk}(t)}(x, y)$ of worn material through an appropriate set of numerical procedure that defines the update strategy. The update strategy is also applied with the aim of reducing the numerical noise characterising the distribution $\delta_{P_{wi}^{jk}(t)}(x, y)$ that can generate problems to the global contact model because of the presence of nonphysical alterations in new profiles.

Another issue to be provided from the update procedure is the average of the worn material distributions. In fact, the output of the wear model must be a single profile; hence, the evaluated distribution $\delta_{P_{wi}^{jk}(t)}(x, y)$ needs to be mediate.

The whole numerical procedure which computes the new profiles can be summed up in the following steps:

1. *Longitudinal integration:*

$$\frac{1}{2\pi w(y_{wi}^{jk})} \int_{-a(y)}^{+a(y)} \delta_{P_{wi}^{jk}(t)}(x, y) dx = \delta_{P_{wi}^{jk}(t)}^{tot}(y); \quad (5)$$

the previous integration provides the mean value of wheel worn material expressed in $\text{mm}^3/(\text{m mm}^2)$. More specifically, the operation sums all the wheel wear contributions in the longitudinal direction inside the contact patch and distributes the resulting quantity along the wheel circumference of length $2\pi w(y_{wi}^{jk})$.

2. *Time integration:*

$$\int_{T_i}^{T_e} \delta_{P_{wi}^{jk}(t)}^{tot}(y) V(t) dt \approx \int_{T_i}^{T_e} \delta_{P_{wi}^{jk}(s_w - s_{wi}^{cjk}(t))}^{tot}(s_w - s_{wi}^{cjk}(t)) V(t) dt = \Delta_{P_{wi}^{jk}}(s_w) \quad (6)$$

where the natural abscissa s_w relative to the curve $w(y_w)$ has been introduced. The following relations locally hold (see Figure 4(a)):

$$y \approx s_w - s_{wi}^{cjk}(t) \quad w(y_w) = w(y_w(s_w)) = \tilde{w}(s_w). \quad (7)$$

The natural abscissa of the contact point s_{wi}^{cjk} can be evaluated starting from its position P_{wi}^{jk} . The integration (6) sums all the wear contributions relative to the dynamic simulation and gives as output the depth of worn material due to the considered contact point $\Delta_{P_{wi}^{jk}}(s_w)$ in $\text{mm} = \text{mm}^3/\text{mm}^2$.

3. *Sum on the contact points:*

$$\sum_{i=1}^{N_{PDC}} \Delta_{P_{wi}^{jk}}(s_w) = \Delta_{jk}^w(s_w) \quad (8)$$

where N_{PDC} represents the maximum number of contact points that can be considered for each single wheel. The output $\Delta_{jk}^w(s_w)$ is the removed material of the j -th wheel during the k -th simulation. The number of active contact points changes during the simulation but it is usually less than N_{PDC} ; thus, the amount of worn material due to non-active contact points is automatically set equal to zero.

4. *Average on the vehicle wheels and on the dynamic simulations:*

$$\sum_{k=1}^{N_c} p_k \frac{1}{N_w} \sum_{j=1}^{N_w} \Delta_{jk}^w(s_w) = \bar{\Delta}^w(s_w) \quad (9)$$

where N_w is the number of vehicle wheels while the p_k , $1 \leq k \leq N_c$, $\sum_{k=1}^{N_c} p_k = 1$ are the statistical coefficients related to the various dynamic simulations. These coefficients have been established by the statistical analysis as will be better explained in the following sections. The average on the number of wheel–rail interactions has to be performed to obtain as output of the wear model a single average profile for the wheel.

5. *Scaling:* Since it normally takes travelled distance of thousands kilometers in order to obtain measurable effects of wheel wear, an appropriate scaling procedure is necessary to reduce the simulated track length with a consequent limitation of the computational effort. The total mileage km_{tot} travelled by the vehicle is chosen according to the purpose of the simulations, for example equal to the re-profiling intervals. This mileage is subdivided into discrete steps characterized by a length equal to km_{step} and the wheel profile is supposed to be constant within each discrete step (corresponding to a travelled distance equal to km_{step}). During this research activity the adaptive step has been adopted for its capacity in representing the nonlinear behaviour of the wear evolution. In the first phase of the simulations, when the interaction between unworn wheel and rail profiles is represented by non-conformal contact, the wear evolution is characterized by a higher rate. In a second phase a slower rate due to the more conformal contact is presented. Furthermore, this strategy presents computational times comparable with those relative to the constant step update strategy. The km_{step} value represents a distance which is still too long to be simulated in reasonable computational times. Assuming that a linear relationship between the amount of worn material and the travelled distance holds within a single step km_{step} of the discrete procedure, it is possible to amplify the quantity of removed material by a suitable scaling factor. The almost linearity characterizing the wear model inside a discrete step (the length of which is defined in this work by means of an adaptive strategy based on a given threshold on maximum value of the cumulated wear depth) represents a working hypothesis coming from the discrete approach of the model. It comes from the idea that the wear rate characterizing the simulated distance km_{prove} (Figure 4) during the considered discrete step remains the same also inside the entire discrete step km_{step} , due to the fact that the vehicle always covers the same railway tracks of the statistical

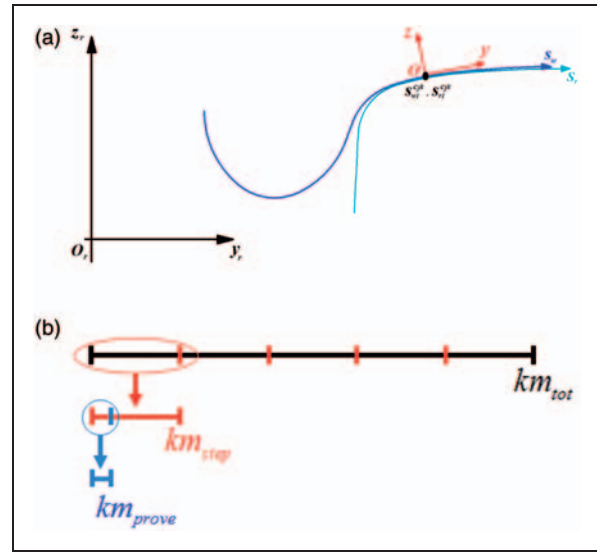


Figure 4. Wear model. (a) normal abscissa for the wheel and rail profile. (b) Discretization of the total mileage.

analysis both during the performed simulations km_{prove} and during the entire discrete step km_{step} . The quantity $\Delta_{max} = \max_{s_w} \bar{\Delta}^w(s_w)$ represents the maximum cumulated wear depth obtained during the performed simulations km_{prove} . Therefore, a smaller distance km_{prove} can be simulated and the relative amount of wheel worn material can be amplified in order to evaluate the worn material distribution relative to a km_{step} travelled distance. The linearity hypothesis is meaningful only if the km_{step} value is low enough to ensure that wheel profile variation (due to wear) inside it can be neglected.

The discrete step value km_{step} can be then defined through the following equation:

$$km_{step} = km_{prove} \frac{\Delta_{fix}}{\Delta_{max}} \quad (10)$$

where $km_{prove} = l_{track}$ is the total travelled distance simulated during the N_c dynamic analysis. The quantity Δ_{fix} is the related chosen threshold value and in this work it is equal to 0.1 mm. The scaled amount $\bar{\Delta}^{wsc}(s_w)$ of worn material to be removed by the wheel surface is then given by the following expression:

$$\bar{\Delta}^{wsc}(s_w) = \bar{\Delta}^w(s_w) \frac{\Delta_{fix}}{\Delta_{max}} \quad (11)$$

6. *Smoothing of the worn material:* the smoothing of the removed material function $\bar{\Delta}^{wsc}(s_w)$ is necessary to remove the numerical noise and short wavelengths without physical meanings that affects this quantity and that would be passed to the new profile $\tilde{w}_n(s_w)$, of wheel causing problems to the global contact models:

$$\mathfrak{S}[\bar{\Delta}^{wsc}(s_w)] = \bar{\Delta}_{sm}^{wsc}(s_w) \quad (12)$$

Hence, an appropriate smoothing of the worn material distributions is required and this is achieved by means of a first-order discrete filter²⁵ (i.e. a moving average filter characterized by a window size equal to 1 % ÷ 5 % of the total number of points in which the profiles are discretised). This kind of discrete filter, characterised by high numerical efficiency and simplicity, permits to conserve the mass of the material removed by wear.

7. Profile update:

$$\begin{pmatrix} y_w(s_w) \\ \tilde{w}_o(s_w) \end{pmatrix} - \bar{\Delta}_{sm}^{wsc}(s_w) \mathbf{n}_w^r \xrightarrow{\text{re-parameterization}} \begin{pmatrix} y_w(s_w) \\ \tilde{w}_n(s_w) \end{pmatrix} \quad (13)$$

the last step of the procedure consists in the determination of the new wheel profile $\tilde{w}_n(s) = w_n(y)$ starting from the old one $\tilde{w}_o(s) = w_o(y)$. Due to the fact that the removal of material occurs in the normal direction to the profiles (\mathbf{n}_w^r is the outgoing unit vector for the wheel profile) once the quantity $\bar{\Delta}_{sm}^{wsc}(s_w)$ has been removed a re-parameterisation of the profile must be performed to get curve parameterised by means of the curvilinear abscissa.

Setting-up of the Minuetto virtual track

This section is a brief overview on the procedure used in deriving a significant statistical track description, an essential task to make possible and rationalize the approach and the simulation work on a complex railway line.

In the present work the statistical approach has been exploited to draw up the mean line of the Minuetto train. This mean line had to be a significant and equivalent synthesis from the wear viewpoint, in a statistical sense, of the whole set of tracks in Italian railways on which the train composition operates every day. The same strategy has also been used in drawing up a virtual track of the Aosta-Pre Saint Didier line aimed at the model validation via comparison with the available experimental results.⁸

The basic idea is to substitute the simulation on the whole track with an equivalent set of simulations on short curved tracks (see Table 2), each one characterized by a length value l_{track} . More precisely, the steps performed to get the statistical representation were the following:

- a set of curve radius intervals characterized by a minimum R_{min} and a maximum R_{max} was identified analyzing the database provided by RFI;
- each of these intervals was furthermore divided in superelevation subclasses, each of them with its own h_{min} and h_{max} ;

- for each subclasses a representative radius R_r was calculated as a weighted average on all the curve radii included in that subclasses, using the length of curve as a weighting factor;
- the corresponding representative superelevation h_r was chosen as the most frequent superelevation among the values found in that class;
- for each subclasses a speed value V_r was chosen as the minimum value between the max speed allowable equal to V_{max} (depending on the radius, the superelevation and vehicle characteristics) and the speed \tilde{V} calculated imposing a non-compensated acceleration of $a_{nc}^{lim} = 0.6 \text{ m/s}^{210,11}$;

$$\frac{\tilde{V}^2}{R_r} - \frac{h_r}{s} g = a_{nc}^{lim} \quad V_r = \min(\tilde{V}, V_{max}) \quad (14)$$

where g is the gravitational acceleration and s is the nominal distance (1500 mm) between the two contact points on the wheelset when it is centered on the track;

- a weighting factor p_k was introduced for each subclass to take into account the frequency of a certain matching radius-superelevation in the track and to diversify the wear contributions of the different curves. This latter ($0 \leq p_k \leq 1$) is computed taking into account the frequency of each subtrack within the whole statistical analysis of the Italian railway net.
- the transition lengths of the real track are incorporated in the constant curvature sections next to them (the inner transition is included in the previous constant curvature section while the outer transition is included in the next one); hence, the wear is numerically evaluated on curves and straight tracks only.

The statistical approach to the Italian mean line has provided the classification shown in Table 2, made up of N_C different classes (33 curves and the straight track). For each one of the N_C classes of curves a different constant average worn rail profile provided by RFI, obviously characterized by a different wear between inner and outer side, has been considered (in Figure 5 are represented the outer rail profiles); particularly, the rail profiles have more severe wear if the curve radius decreases because of the worse contact conditions characterising the wheel-rail pairs. Finally, at this phase of the research, track irregularities have not been considered.

Description of the proposed wheel profile and of the optimisation procedure

This section describes the procedures for the design/optimisation of the DR2 wheel profile. This procedure has been developed by the authors⁵ in order to improve the poor performance with regard to the resistance to wear and the guidance in sharp curves

Table 2. The Minuetto virtual track.

N_C	R_{min} (m)	R_{max} (m)	R_r (m)	$h_{min} - h_{max}$ (mm)	h_r (mm)	V_r (km h ⁻¹)	p_k (%)
1	250	278	263	90-120	90	65	1.90
2				130-160	160	75	4.21
3	278	313	294	90-120	90	70	1.11
4				130-160	160	80	1.62
5	313	357	333	90-120	90	70	0.44
6				130-160	140	80	1.24
7	357	417	385	50-80	50	70	0.80
8				90-120	120	80	1.33
9				130-160	150	90	4.17
10	417	500	455	50-80	80	70	1.44
11				90-120	100	80	4.72
12				130-160	130	90	1.29
13	500	625	556	10-40	10	70	0.14
14				50-80	80	80	1.52
15				90-120	90	85	2.01
16				130-160	150	110	1.46
17	625	833	714	10-40	10	70	0.09
18				50-80	70	85	1.56
19				90-120	90	95	1.77
20				130-160	130	115	0.78
21	833	1250	1000	10-40	10	70	1.10
22				50-80	50	85	2.41
23				90-120	120	130	2.16
24				130-160	140	130	0.93
25	1250	2500	1667	0	0	70	0.17
26				10-40	30	85	1.91
27				50-80	80	130	1.68
28				90-120	90	130	0.99
29				130-160	150	130	0.17
30	2500	10000	5000	0	0	70	1.08
31				10-40	20	120	1.21
32				50-80	50	130	0.25
33				90-120	100	130	0.004
34			∞			130	52.3

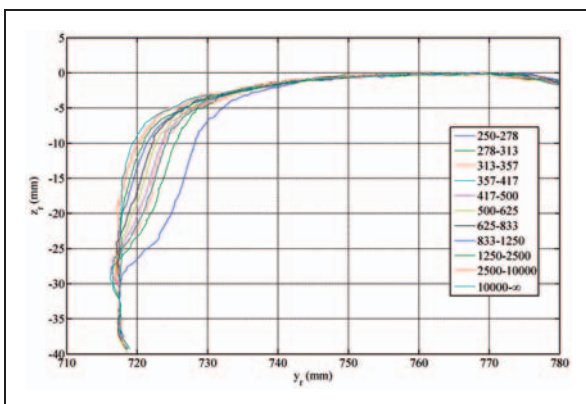


Figure 5. External worn rail profile of each class (cant of 1/20 rad).

that the S1002 wheel profile, originally designed to match the UIC60 rail profile canted at 1/40 rad exhibits when coupled to the UIC60 rail profile canted at 1/20 rad.

DR2 wheel profile

The design of the DR2 wheel profile aims to guarantee the kinematic characteristics of the original matching formed by ORE S1002 wheel profile and UIC60 rail profile with inclination angle α_p equal to 1/40 rad, also with the new matching DR2 wheel profile – UIC60 rail profile canted at 1/20 rad. The kinematic properties of the original matching have been chosen as reference value, because it is widely common in

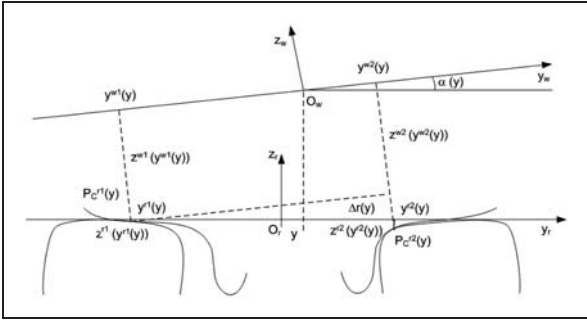


Figure 6. Adopted nomenclature for DR2 design.

European railways and it is characterised by good performances in both wear and kinematic behaviour.

The procedure developed by the authors to design the DR2 wheel profile is articulated in several steps. A first intermediate wheel profile, conventionally named DR1, is designed according to the purposes previously described. The resulting rolling radii difference (RRD) function (the difference between rolling radii of the right and the left wheels for each lateral displacement y), is then compared with the one characterising the original wheel and rail profiles matching and an RRD error function is obtained. The minimization of the error function through an appropriate algorithm leads then to the optimised version of the wheel profile, conventionally named DR2.

The design of the DR2 profile requires the introduction of two appropriate reference systems, namely the rail (or auxiliary) reference system O_r, x_r, y_r, z_r and the wheel (or local) reference system O_w, x_w, y_w, z_w , both shown in Figure 6. The longitudinal axis x_r of the rail reference system is built tangent to the track centerline in the point O_r , while the z_r axis is normal to the top of rails plane. The origin O_w of the wheel reference system coincides with the center of mass G_w of the wheelset. The x_w axis is parallel to the x_r axis and the y_w axis is coincident with the rotation axis of the wheelset.

The position of the wheel reference system origin expressed in the rail reference system is denoted by $O_w^r = [y \quad z(y)]^T$ and the orientation matrix is R :

$$R = \begin{bmatrix} \cos \alpha(y) & -\sin \alpha(y) \\ \sin \alpha(y) & \cos \alpha(y) \end{bmatrix} \quad (15)$$

Introducing apices 1 and 2 to denote respectively the right and left wheel, the coordinates of the contact points respectively in the auxiliary reference and the local reference system may be defined as

$$\begin{aligned} \mathbf{P}_c^{r1} &= [y^{r1}(y) \quad z^{r1}(y^{r1}(y))]^T \\ \mathbf{P}_c^{r2} &= [y^{r2}(y) \quad z^{r2}(y^{r2}(y))]^T \\ \mathbf{P}_c^{w1} &= [y^{w1}(y) \quad z^{w1}(y^{w1}(y))]^T \\ \mathbf{P}_c^{w2} &= [y^{w2}(y) \quad z^{w2}(y^{w2}(y))]^T. \end{aligned} \quad (16)$$

Design of the DR1 wheel profile. In the present research activity, the purpose in maintaining the kinematic properties of the ORE S1002-UIC60 canted at $1/40$ rad matching is achieved by imposing that some variables of the new matching (DR2 wheel profile – UIC60 matching canted at $1/20$ rad) remain the same of the original ones. More specifically, these variables (all depending on the wheelset lateral displacement y) are the lateral coordinates y_{r1}, y_{r2} of the contact points expressed in the auxiliary reference system, the old rail functions $z_{40}^{r1}(y_{40}^{r1}), z_{40}^{r2}(y_{40}^{r2})$, the vertical coordinate $z(y)$ and the roll angle $\alpha(y)$ of the wheelset. Taking into account the roll angle of the wheelset, which is small if compared, for example, with the cant angle, does not adversely influence the stiffness and ill-conditioning of the problem thanks to the robustness of the algorithm. In the remaining of the article the variables characterising the original matching and those referring to the new matching will be respectively denoted with the subscripts 40 and 20.

Consequently, the six inputs required by the design procedure from the old matching are $y_{40}^{r1}(y), y_{40}^{r2}(y), \alpha_{40}(y), z_{40}^r(y), z_{40}^{r1}(y_{40}^{r1}), z_{40}^{r2}(y_{40}^{r2})$ while the two further inputs required from the new matching are $z_{20}^{r1}(y_{40}^{r1}), z_{20}^{r2}(y_{40}^{r2})$.

The DR1 wheel profile design procedure is formed by several steps. Starting from these inputs, the equations describing the coordinate transformation of the contact points between the local and the auxiliary reference system can be written both for the original matching:

$$\begin{pmatrix} y_{40}^{r1}(y) \\ z_{40}^{r1}(y_{40}^{r1}(y)) \end{pmatrix} = \begin{pmatrix} y \\ z_{40}(y) \end{pmatrix} + R(\alpha_{40}(y)) \begin{pmatrix} y_{40}^{w1}(y) \\ z_{40}^{w1}(y_{40}^{w1}(y)) \end{pmatrix} \quad (17)$$

$$\begin{pmatrix} y_{40}^{r2}(y) \\ z_{40}^{r2}(y_{40}^{r2}(y)) \end{pmatrix} = \begin{pmatrix} y \\ z_{40}(y) \end{pmatrix} + R(\alpha_{40}(y)) \begin{pmatrix} y_{40}^{w2}(y) \\ z_{40}^{w2}(y_{40}^{w2}(y)) \end{pmatrix} \quad (18)$$

and for the new matching:

$$\begin{pmatrix} y_{40}^{r1}(y) \\ z_{20}^{r1}(y_{40}^{r1}(y)) \end{pmatrix} = \begin{pmatrix} y \\ z_{40}(y) \end{pmatrix} + R(\alpha_{40}(y)) \begin{pmatrix} y_{20}^{w1}(y) \\ z_{20}^{w1}(y_{20}^{w1}(y)) \end{pmatrix} \quad (19)$$

$$\begin{pmatrix} y_{40}^{r2}(y) \\ z_{20}^{r2}(y_{40}^{r2}(y)) \end{pmatrix} = \begin{pmatrix} y \\ z_{40}(y) \end{pmatrix} + R(\alpha_{40}(y)) \begin{pmatrix} y_{20}^{w2}(y) \\ z_{20}^{w2}(y_{20}^{w2}(y)) \end{pmatrix} \quad (20)$$

where the wheelset lateral displacement value y is bounded in the range $[-y_M, y_M]$. The wheel profiles optimisation procedure has been performed for a maximum lateral displacement equal to $y_M = 10$ mm. Usually, the clearance value varies between 10 mm and 15 mm depending on the track gauge value (in this case it is equal to 1435 mm), on the rail inclination angle and on the wheelset width (in this case it is equal to 1500 mm). Hence, the maximum

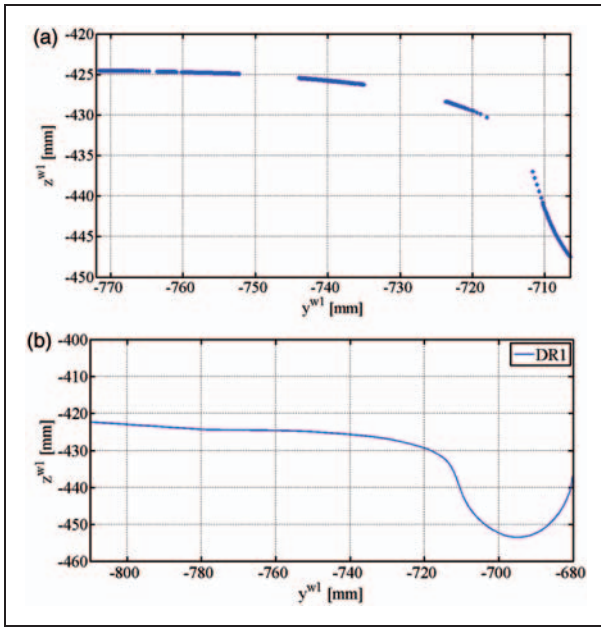


Figure 7. DRI wheel profile design. (a) Contact points distribution. (b) DRI wheel profile.

semi-clearance is equal to 7.5 mm. Thereby, in order to consider all the possible operating range of lateral wheelset displacement, we chose an y_M value equal to 10 mm.

The outputs of the design procedure that characterise the new wheel profile are the lateral $y_{20}^{w1}(y)$, $y_{20}^{w2}(y)$ and vertical $z_{20}^{w1}(y_{20}^{w1}(y))$, $z_{20}^{w2}(y_{20}^{w2}(y))$ coordinates of the contact points of the new wheel profile in the local reference system. The design procedure is performed in a discrete way for every y value of the discretised range $[-y_M, y_M]$ (with a resolution equal to 0.1 mm).

The profile resulting from the previous step is characterised by gaps (see Figure 7(a)), that are regions where there is not any computed contact point. In the present procedure these regions have been filled fitting the computed points with spline functions and the resulting wheel profile, named DR1, is illustrated in Figure 7(b).

The RRD functions characterising the original (ORE S1002 wheel profile and UIC60 canted at 1/40 rad) and the resulting matching are respectively defined through the following expressions (Figure 8):

$$\begin{aligned} \Delta r_{40} &= z_{40}^{w2}(y_{40}^{w2}(y)) - z_{40}^{w1}(y_{40}^{w1}(y)) \\ \Delta r_{20} &= z_{20}^{w2}(y_{20}^{w2}(y)) - z_{20}^{w1}(y_{20}^{w1}(y)). \end{aligned} \quad (21)$$

The adopted design procedure implies that the RRD of the output matching is equal to the one characterising the original matching, disregarding a small estimable variation $e = \Delta r_{20} - \Delta r_{40}$ (see Figure 9), calculated by means of an appropriate analytical procedure.

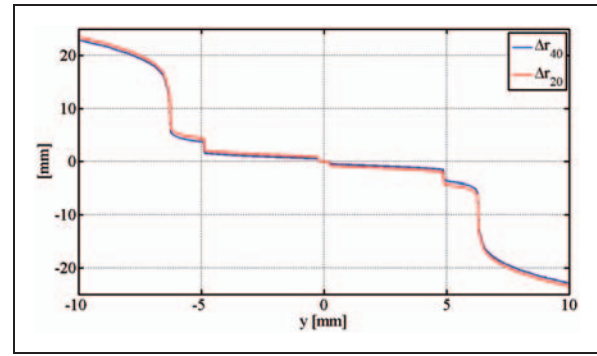


Figure 8. Rolling radii differences: $\Delta_{00A0}r_{20} = z_{20}^{w2}(y_{20}^{w2}(y)) - z_{20}^{w1}(y_{20}^{w1}(y))$ relative to the matching DRI-UIC60 canted at 1/20 rad and $\Delta_{00A0}r_{40} = z_{40}^{w2}(y_{40}^{w2}(y)) - z_{40}^{w1}(y_{40}^{w1}(y))$ relative to the ORE S1002-UIC 60 rail canted at 1/40 rad.

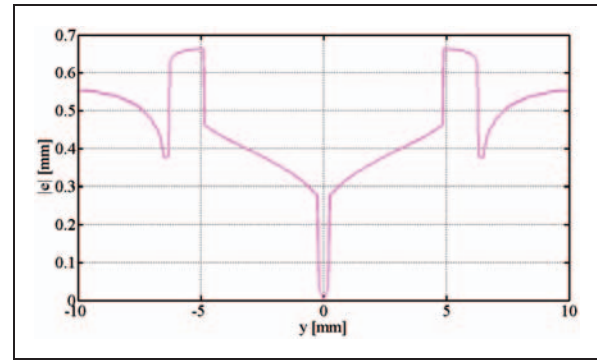


Figure 9. Absolute value of the error e in rolling radii difference distribution for the DRI-UIC60 canted at 1/20 rad matching.

Optimisation of the wheel profile and design of DR2 wheel profile. In order to improve the RRD error between the original matching and DR1 wheel profile, UIC60 canted at 1/20 rad matching, an optimisation algorithm has been developed according to the following procedure.

An expression of the RRD functions variation between the new and the original matching can be obtained. Subtracting equation 17 from equation 18 and equation 19 from equation 20 leads to the following expressions:

$$\begin{aligned} &\begin{pmatrix} y_{40}^{r2}(y) - y_{40}^{r1}(y) \\ z_{40}^{r2}(y_{40}^{r2}(y)) - z_{40}^{r1}(y_{40}^{r1}(y)) \end{pmatrix} \\ &= R(\alpha_{40}) \begin{pmatrix} y_{40}^{w2}(y) - y_{40}^{w1}(y) \\ \Delta r_{40} \end{pmatrix} \end{aligned} \quad (22)$$

$$\begin{aligned} &\begin{pmatrix} y_{20}^{r2}(y) - y_{20}^{r1}(y) \\ z_{20}^{r2}(y_{20}^{r2}(y)) - z_{20}^{r1}(y_{20}^{r1}(y)) \end{pmatrix} \\ &= R(\alpha_{40}) \begin{pmatrix} y_{20}^{w2}(y) - y_{20}^{w1}(y) \\ \Delta r_{20} \end{pmatrix}. \end{aligned} \quad (23)$$

Then, subtracting equation 22 from equation 23 it holds:

$$R_{(\alpha_{40})}^T \begin{pmatrix} 0 \\ \Delta z_{20}^r - \Delta z_{40}^r \end{pmatrix} = \begin{pmatrix} \Delta y_{20}^r - \Delta y_{40}^r \\ \Delta r_{20} - \Delta r_{40} \end{pmatrix}. \quad (24)$$

The second component of the previous equation leads to the expression of the rolling radii functions variation between the new and the original matching

$$(\Delta z_{20}^r - \Delta z_{40}^r) \cos \alpha_{40} = \Delta r_{20} - \Delta r_{40} = e(y) \quad (25)$$

as a function of the wheelset lateral displacement where

$$\begin{aligned} \Delta z_{20}^r &= z_{20}^{r2}(y_{40}^{r2}(y)) - z_{20}^{r1}(y_{40}^{r1}(y)) \text{ and} \\ \Delta z_{40}^r &= z_{40}^{r2}(y_{40}^{r2}(y)) - z_{40}^{r1}(y_{40}^{r1}(y)). \end{aligned}$$

The basic idea of this algorithm consists in translating the lateral input coordinates $y_{40}^{r1}(y)$, $y_{40}^{r2}(y)$ of a certain quantity $k(y)$, evaluated through a minimisation process of the RRD function error for each possible lateral wheelset displacement y . The lateral coordinates of the contact points in the auxiliary reference system can be then re-defined as:

$$y_{40}^{r1}k = y_{40}^{r1} + k \quad y_{40}^{r2}k = y_{40}^{r2} + k \quad (26)$$

where the k value is bounded in the range $[-\bar{k}, +\bar{k}] = I_k$. Therefore, the expression of the rolling radii error (equation 25) becomes a function of both y and k values:

$$E(y, k) = \cos \alpha_{40} (z_{20}^{r2}(y_{40}^{r2} + k) - z_{20}^{r1}(y_{40}^{r1} + k) - z_{40}^{r2}(y_{40}^{r2}) + z_{40}^{r1}(y_{40}^{r1})). \quad (27)$$

Equation 27 is used as the objective function to find the optimal value k_{opt} of the translation quantity, which is then defined for each wheelset lateral displacement y as:

$$k_{opt}(y) = \arg \min_{k \in I_k} |E(y, k)|. \quad (28)$$

The optimisation process is performed by discretising the I_k range with a resolution equal to 0.1 mm.

Figure 10(a) illustrates the graphical representation of the k_{opt} value for a determined lateral displacement y . The resulting lateral coordinates of the contact points in the auxiliary reference system are evaluated as:

$$y_{opt}^{r1} = y_{40}^{r1} + k_{opt} \quad y_{opt}^{r2} = y_{40}^{r2} + k_{opt}. \quad (29)$$

It should be noticed that the optimal shift values k_{opt} of the contact points do not necessarily need to be small. The important thing is that they provide reasonable values of y_{opt}^r contained inside the existence

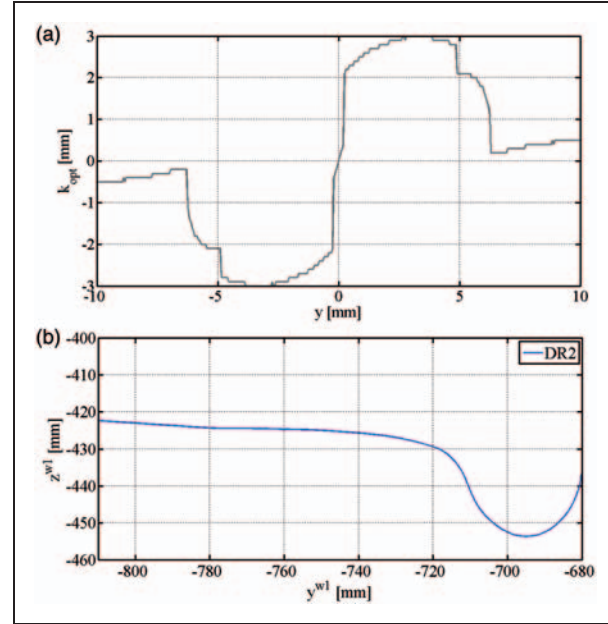


Figure 10. DR2 wheel profile design. (a) Optimal value of the translation quantity k . (b) DR2 wheel profile.

domain limits of the rail function $z_{20}^r(y_{20}^r)$ (which is known).

Through the introduction of the resulting coordinates into equation 20 and equation 19, the outputs $y_{20}^{w1}(y)$, $z_{20}^{w1}(y_{20}^{w1}(y))$, $y_{20}^{w2}(y)$, $z_{20}^{w2}(y_{20}^{w2}(y))$ of the optimised wheel profile-UIC60 rail canted at 1/40 rad matching are given by the following expressions:

$$\begin{aligned} \begin{pmatrix} y_{opt}^{r1}(y) \\ z_{20}^{r1}(y_{opt}^{r1}(y)) \end{pmatrix} &= \begin{pmatrix} y \\ z_{40}(y) \end{pmatrix} \\ &+ R(\alpha_{40}(y)) \begin{pmatrix} y_{20}^{w1}(y) \\ z_{20}^{w1}(y_{20}^{w1}(y)) \end{pmatrix} \end{aligned} \quad (30)$$

$$\begin{aligned} \begin{pmatrix} y_{opt}^{r2}(y) \\ z_{20}^{r2}(y_{opt}^{r2}(y)) \end{pmatrix} &= \begin{pmatrix} y \\ z_{40}(y) \end{pmatrix} \\ &+ R(\alpha_{40}(y)) \begin{pmatrix} y_{20}^{w2}(y) \\ z_{20}^{w2}(y_{20}^{w2}(y)) \end{pmatrix}. \end{aligned} \quad (31)$$

The optimised wheel profile, obtained after the gaps fitting procedure and named DR2 wheel profile, is shown in Figure 10(b).

The new RDD function is compared with the original one in Figure 11; it shows that the two plots are almost coincident and that the error (see Figure 12), which depends on the discretisation precision of the range I_k , is about zero.

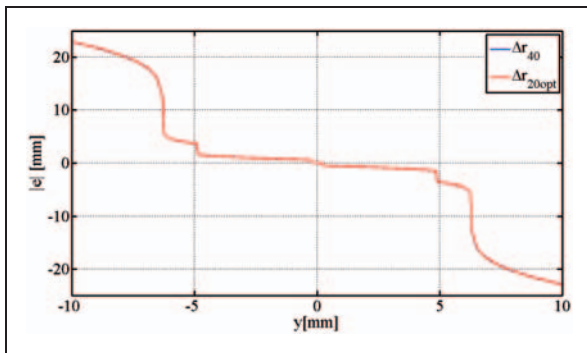


Figure 11. Rolling radii differences: $\Delta r_{20} = z_{20}^{w2}(y_{20}^{w2}(y)) - z_{20}^{w1}(y_{20}^{w1}(y))$ relative to the optimised matching DR2-UIC60 canted at $1/20$ rad and $\Delta r_{40} = z_{40}^{w2}(y_{40}^{w2}(y)) - z_{40}^{w1}(y_{40}^{w1}(y))$ relative to the ORE S1002-UIC 60 rail canted at $1/40$ rad.

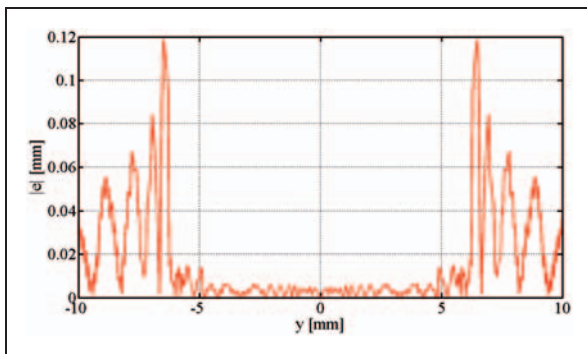


Figure 12. Absolute value of the error e in rolling radii difference distribution for the DR1-UIC60 canted at $1/20$ rad matching.

The design procedure adopted to define the DR2 discrete wheel profile may be affected by numerical errors coming from different sources such as:

- use of splines in the gaps (where there is not a contact point distribution) and of fictitious points at the extremities of the wheel profile (parts of the ORE S1002 have been used);
- subsequent re-interpolations and smooth process of profiles and derivatives of the wheel and the rail;
- since the DR2 wheel profile and UIC60 rail canted at $1/20$ rad matching is based on the geometrical properties of the ORE S1002-UIC60 canted at $1/40$ rad, it is characterised by the stiffness caused by the conformal contact typical of the original matching. In fact, as long as the contact becomes more conformal, contact points move more quickly along the contact surfaces even for small variations of the surfaces relative positions, leading to an increase in stiffness and ill-conditioning of the problem;
- the resulting DR2 wheel profile is smooth and consequently it does not lead to dynamical problems due to non-smooth derivatives.

At the same time, one of the numerical advantage of the procedure consists in the fact that the new DR2

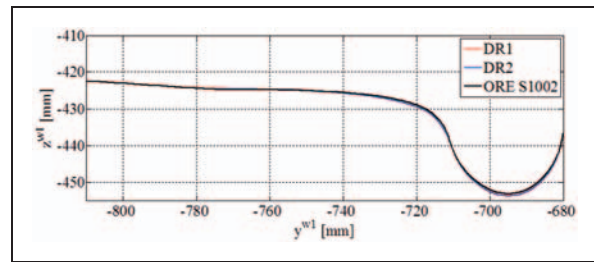


Figure 13. DRI, DR2 and ORE S1002 wheel profiles.

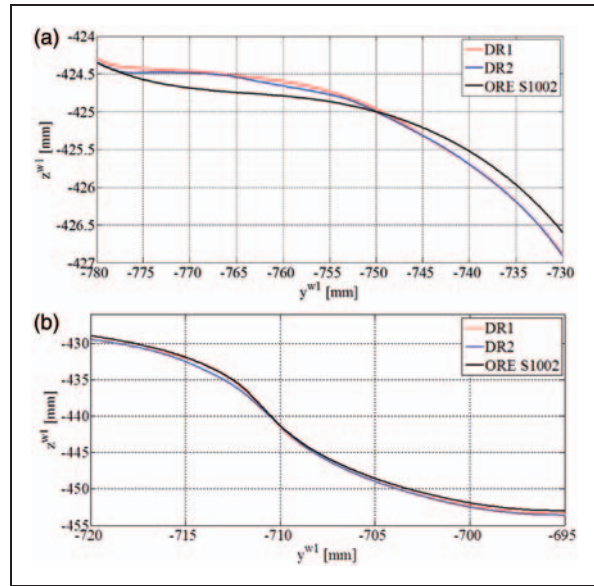


Figure 14. Comparison of the three wheel profiles. (a) Tread zone. (b) Flange zone.

wheel profile is designed without any condition on the derivatives of the profiles; this aspect involves a reduction of the smoothing requirements and does not further increase the ill-conditioning characteristic of the design problem.

Comparison between the resulting wheel profiles

This section deals with the comparison of the DR1 and DR2 characteristics with those relative to the standard ORE S1002 (optimised to match the UIC60 rail canted at $1/40$ rad). Figure 13 shows the comparison between the resulting DR1 and DR2 wheel profiles and the original ORE S1002, while in Figure 15 their relative differences along the vertical coordinates are plotted.

The derivatives of the resulting DR1 and DR2 wheel profile compared with the derivative of the standard ORE S1002 are illustrated in Figure 16.

The DR1 and DR2 wheel profiles are almost similar, representing that the DR2 optimisation algorithm may improve the DR1 designing procedure which nevertheless, produces itself a wheel profile with good kinematic and wear characteristics. It can be noticed that the new DR1 and DR2-UIC60 canted at $1/20$ matching try to reproduce the conformal

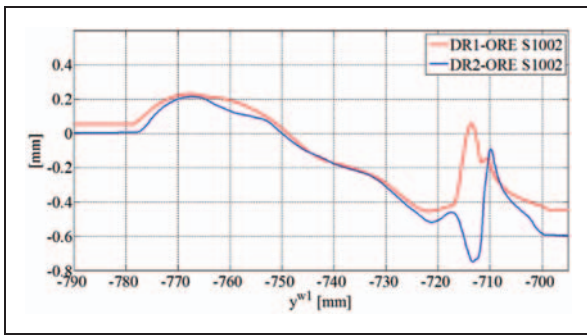


Figure 15. Vertical differences DR1-ORE S1002 and DR2-ORE S1002.

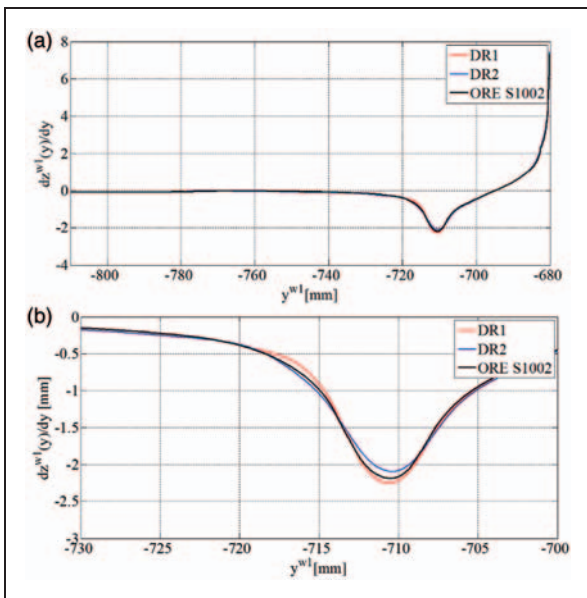


Figure 16. DR1, DR2 and ORE S1002 wheel profile derivatives.

contact characterizing the original matching ORE S1002-UIC60 canted at 1/40 with coherent vertical translations of the wheel profiles and derivatives in the tread and flange zone. More specifically, the points of the new wheel profiles in the tread zone (Figure 14(a)) are translated upwards with respect to those characterising the original ORE S1002 wheel profile, while the points in the flange zone slope downwards (Figure 14(b)).

Wear control parameters

According to the current European Standard EN 15313,¹¹ the wear condition in a wheel can be evaluated through the measurement of three particular dimensions (the qR quota, the flange thickness fT and the flange height fH , without a complete detection of the 2D profile. The adopted nomenclature for the definition of the aforementioned quotas is shown in Figure 17).

It must be noticed that other effects (hollow wear, rolling radius difference) cannot be estimated through

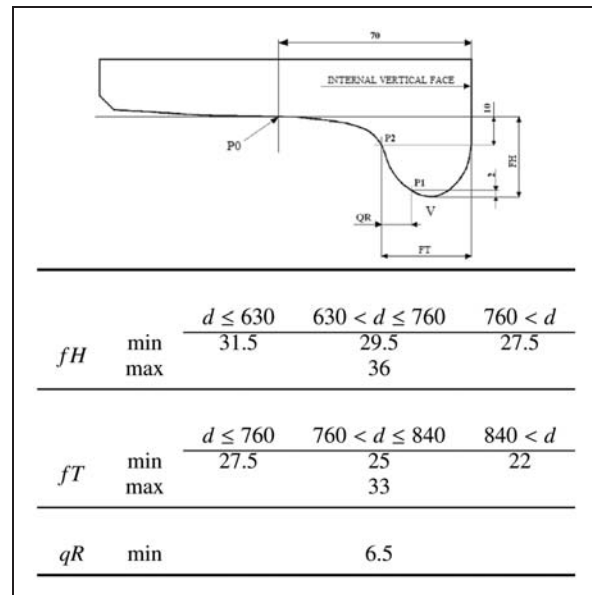


Figure 17. Reference dimensions of the wheel profile (left) and limit values in mm (right) for a wheel having an actual rolling diameter equal to d .

the simple evaluation of the standard reference dimensions: These effects have not been taken into account in the present phase of the research activity due to the unavailability of specific experimental data.

The point P0 on the profile is 70 mm distant from the internal side of the wheel, the point P1 is 2 mm above the lowest point V of the flange on the wheel profile and the point P2 is 10 mm below P0 on the profile. The flange thickness fT is defined as the distance between P2 and the internal vertical side of the wheel; the qR is the horizontal distance between P1 and P0; the flange height fH is the vertical distance between P0 and V. P0 is also the point where the conventional rolling radius of a wheel is taken.

Because of the way the quotas are defined, they are positive and do not depend on the wheel rolling radius. The values of these parameters are measured periodically in order to decide whether the profile has to be re-turned or not (if it is still possible), considering the maximum or minimum values suggested by the current standard.¹¹ These limit values are reported in Figure 17. With regard to their physical meaning, both the flange thickness fT and the flange height fH describe the size of the flange: variations of the first quota are due to the action of the wear which progressively reduces the thickness of the flange and its structural resistance, while the rise of the flange height is a measure of the wear on the tread. Conversely, the qR dimension is a shape parameter which quantifies the local conicity on the flange. The check of the wheel wear parameters enables the prediction of the consequences that wheel profiles wear determines on the dynamic behavior of the railway vehicles. Even if running performances of a rail vehicle are ruled by the entire wheel–rail coupling and

interaction, the control of wheel wear evolution (according to current standards) represents an important aspect to avoid wear, stability or guidance problems.

Wear analysis

In this section, the results of the dynamic simulations aimed at a wear evaluation will be presented in order to compare the profiles considered in this study: the standard S1002 and the DR2 wheel profiles. The simulation campaign has been performed considering the compared wheel profiles running on the same rail inclination 1/20 rad. Concerning the resistance to wear, the performance can be assessed by analysing the evolution of three reference dimensions introduced in section “Wear control parameters”.

To this end, Figure 18 shows the progress of the mean qR dimension for each profile: as can be seen, the progress of DR2 profile is slower than that of the S1002. In fact, assuming a comparison limit equal to

7 mm, which is slightly above than the acceptable threshold value of 6.5 mm prescribed by the standard,¹¹ the trend of the DR2 shows that the comparison limit is reached with an increase in the covered distance by at least 30%.

With regard to the progress of the flange thickness fT depicted in Figure 19, the minimum value equal to 22 mm¹¹ is reached after covering about 80,000 km when the S1002 profile is adopted on the Minuetto; differently, with the new profiles the total covered distance can be extended up to 100,000 km and above. Regarding the flange height fH , the comparison is depicted in Figure 20: this quota usually increases owing to the wear on the tread of the profile. However, in the case of study the wear is specially localized on the wheel flange and the consequent slight increase of the flange height is not critical regarding the wear evolution progress. Obviously, it is not true when the tread wear is dominating: to this aim other experimental tests are currently being performed to obtain data also for tread wear progress (to get this data more time and kilometers are needed). The progress of the quotas shows also a relocation of the material towards the tread zone.

With respect to the evolution of the wheel shape, the comparison between the initial and the final condition for the ORE S1002 and DR2 profiles is presented in Figures 21 and 22. The variation in wheel

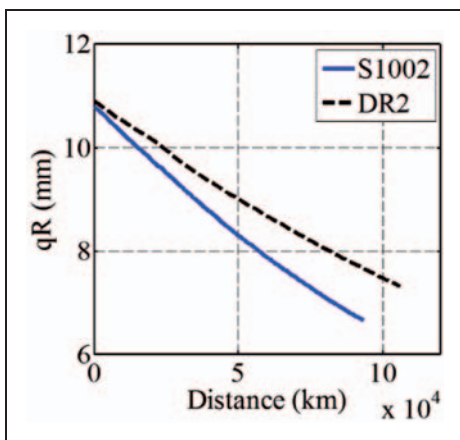


Figure 18. Progress of the qR dimension: comparison of the wheel profiles.

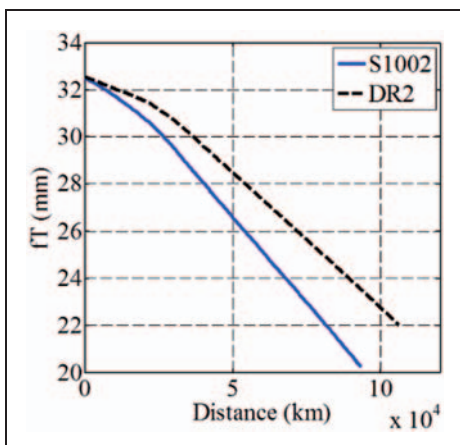


Figure 19. Progress of the fT dimension: comparison of the wheel profiles.

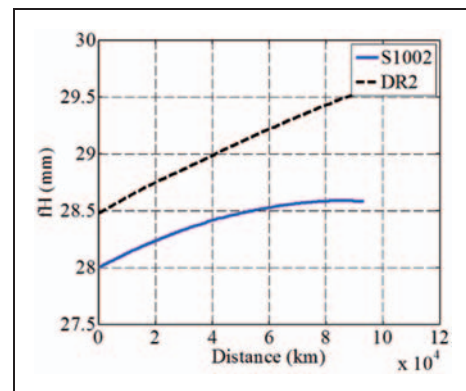


Figure 20. Progress of the fH dimension: comparison of the wheel profiles.

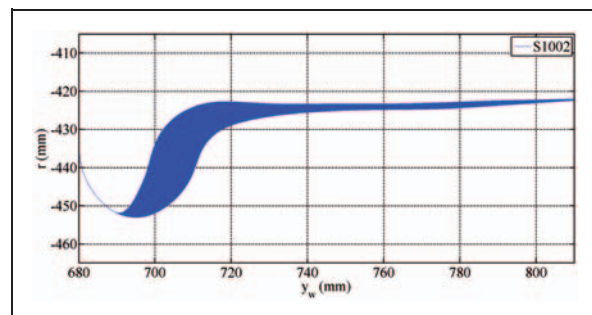


Figure 21. Evolution of the S1002 wheel profile due to wear.

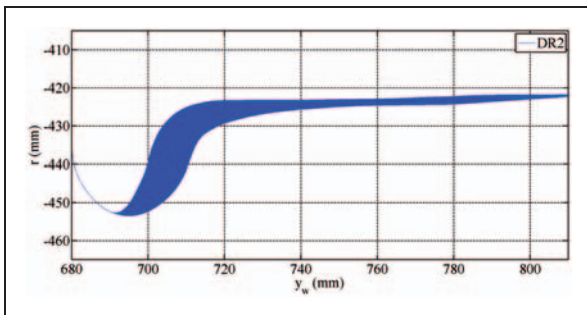


Figure 22. Evolution of the DR2 wheel profile due to wear.

profile is numerically described by means of about 100 procedure steps and besides the worn and the final profile, all the intermediate wheel geometries have also been plotted in the relative figure. Since the mean line of the Minuetto comprises a relevant percentage of sharp curves, the wear is mainly located on the flange instead of the tread. The DR2 wheel shape evolution shows a relocation of the worn material towards the tread zone respect to the standard ORE S1002 shape evolution; it indicates a better and more uniform distribution of the worn material along the profiles that leads to an increase of the wheel profile life.

Conclusions

In this paper, the authors presented a work focused on the development of a mathematical model for the wheel–rail wear evaluation in complex rail networks and on the comparison between the performance provided by different wheel profiles, developed through an analytical optimisation procedure, in terms of resistance to wear. More precisely, the standard ORE S1002 wheel profile, which is widely used on vehicles in service on the Italian railways, has been compared with an innovative wheel profile developed by authors to improve the poor performance with regard to the resistance to wear that the S1002 wheel profile exhibits when matched to the UIC60 rail profile canted at $1/20$ rad). The activity has been performed in collaboration with Trenitalia S.p.A and Rete Ferroviaria Italiana which provided the necessary technical and experimental data for the implementation of the whole wear evaluation procedure.

The developed architecture is based on the mutual interaction between two main parts: a *vehicle model* responsible for the vehicle dynamics and a *wear model* for the evaluation of the amount and the distribution of material to be removed on wheels. The interaction between the vehicle dynamics and the wear model occurs at discrete steps and the evolution of the wheel geometry is reproduced through several intermediate profiles.

The entire procedure was validated in a previous work^{8,9} by means of the experimental data, provided by Rete Ferroviaria Italiana, regarding to the Aosta

Pre-Saint Didier track and the ALn 501 “Minuetto vehicle”.

The developed model has been used in this work for a wear assessment on the ALn 501 Minuetto taking into account the whole Italian railway net in which these vehicles operate. The wear progress has been simulated on an equivalent statistical model of the complex railway, built by consulting the detailed database provided by Rete Ferroviaria Italiana.

The innovative wheel profile developed in this activity for the UIC60 rail with a cant of $1/20$ rad has proven to work fine as regards the resistance to wear if compared with the S1002 wheel profile, both in terms of reference quotas and of the overall profile.

Future developments of the present work will be based first of all on the experimental evaluation of the wear on the Minuetto equipped with wheelsets having the new wheel profile by means of experimental tests that have been scheduled by Trenitalia, in order to verify the response in terms of progress of the reference dimensions. Furthermore, track irregularities associated to each curve class will be considered; these irregularities will be chosen thanks to the new experimental data provided from Trenitalia S.p.A. Finally, other experimental tests are currently being performed to obtain data also for tread wear progress.

Funding

This research received no specific grant from any funding agency in the public, commercial, or not-for-profit sectors.

Conflict of interest

None declared.

Acknowledgements

The authors would like to thank Engg. R. Cheli, G. Grande and R. Desideri of Trenitalia S.p.A. for providing the data relative to the ALn 501 Minuetto vehicle and for their technical support during the whole research activity. A special thanks also goes to the Engg. R. Mele and M. Finocchi of Rete Ferroviaria Italiana for the data relative to the Italian railway lines on which the Minuetto vehicle operates.

References

1. Polach O. Wheel profile design for target conicity and wide tread wear spreading. *Wear* 2011; 271: 195–202.
2. Esveld C, Markine V and Shevtsov IY. Shape optimization of a railway wheel profile. *Eur Rail Rev* 2006; 12: 81–86.
3. Zakharov S, Goryacheva I, Bogdanov V, et al. Problems with wheel and rail profiles selection and optimization. *Wear* 2008; 265: 1266–1272.
4. Persson I and Iwnicki S. Optimisation of railway wheel profiles using a genetic algorithm. In: *Proceedings of the 18th international association for vehicle system dynamics symposium*, Kanagawa, Japan.
5. Toni P. *Optimisation of wheel profiles on rails canted at 1/20*. Technical Report, Trenitalia S.p.A., 2010.

6. EN 13715: Railway applications – wheelsets and bogies – wheels – tread profile, 2010.
7. EN 13674-1: Railway applications – track — rail part 1: Vignole railway rails 46 kg/m and above, 2011.
8. Ignesti M, Malvezzi M, Marini L, et al. Development of a wear model for the prediction of wheel and rail profile evolution in railway systems. *Wear* 2012; 284-285: 1–17.
9. Auciello J, Ignesti M, Malvezzi M, et al. Development and validation of a wear model for the analysis of the wheel profile evolution in railway vehicles. *Vehicle Syst Dyn* 2012; 50: 1707–1734.
10. EN 14363: Railway applications – testing for the acceptance of running characteristics of railway vehicles – testing of running behaviour and stationary tests, 2005.
11. EN 15313: Railway applications – In-service wheelset operation requirements – In-service and off-vehicle wheelset maintenance, 2010.
12. Specht W. Beitrag zur rechnerischen Bestimmung des Rad- und Schienenverschleisses durch Gueterwagen Diss, RWTH Aachen, 1985.
13. Auciello J, Meli E, Falomi S, et al. Dynamic simulation of railway vehicles: wheel/rail contact analysis. *Vehicle Syst Dyn* 2009; 47: 867–899.
14. Meli E, Falomi S, Malvezzi M, et al. Determination of wheel – rail contact points with semianalytic methods. *Multibody Syst Dyn* 2008; 20: 327–358.
15. Kalker JJ. *Three-dimensional elastic bodies in rolling contact*. Dordrecht, the Netherlands: Kluwer Academic Publishers, 1990.
16. Kalker JJ. Survey of wheel-rail rolling contact theory. *Vehicle Syst Dyn* 1979; 8: 317–358.
17. Hertz H. The contact of elastic solids. *J Reine Angew Math* 1881; 92: 156–171.
18. Braghin F, Lewis R, Dwyer-Joyce RS, et al. A mathematical model to predict railway wheel profile evolution due to wear. *Wear* 2006; 261: 1253–1264.
19. Enblom R and Berg M. Simulation of railway wheel profile development due to wear influence of disc braking and contact environment. *Wear* 2005; 258: 1055–1063.
20. Pombo J, Ambrosio J, Pereira M, et al. A study on wear evaluation of railway wheels based on multibody dynamics and wear computation. *Multibody Syst Dyn* 2010; 24: 347–366.
21. Pearce TG and Sherratt ND. Prediction of wheel profile wear. *Wear* 1991; 144: 343–351.
22. Zobory I. Prediction of wheel/rail profile wear. *Vehicle Syst Dyn* 1997; 28: 221–259.
23. Borgeaud G. *Die Fhrung des Fahrzeugs im Gleise und die Vorgnge zwischen Rad und Schiene*. Berlin, Germany: Springer, 1973.
24. Kalker JJ. A fast algorithm for the simplified theory of rolling contact. *Vehicle Sys Dyn* 1982; 11: 1–13.
25. Oppenheim A and Schafer RW. *Discrete-time signal processing*. Englewood Cliffs, NJ: Prentice-Hall, 1989.

Appendix

Notations

fH	flange height
fT	flange thickness
h	superelevations of the curvilinear tracks
I_w	wear index
km_{prove}	mileage related to the simulated tracks
km_{step}	mileage related to the discrete adaptive steps
km_{tot}	total investigated mileage
K_W	wear rate
M_{sp}	contact spin moment
n	outgoing vectors of the profiles
N	contact normal force
N_C	number of curvilinear tracks
O_{xyz}	reference systems
p_k	statistical weights
p_n	normal contact pressure
p_t	tangential contact pressures
P	contact points
qR	qR reference quota
r	rail profile
R	radii of the curvilinear tracks
R	orientation matrix
s	rail gauge
s	local slips
T	contact tangential forces
V	vehicle velocity
w	wheel profile
α_p	rail inclination angle
Δ_{fix}	threshold of cumulative wear depth
Δ_{max}	maximum cumulative wear depth
	simulated
ϵ	global creepages

Indices and apexes

i	index related to number of contact points
j	index related to number of vehicle wheels
k	index related to number of dynamical simulations
r	index related to rail parameters
w	index related to wheel parameters
1	index related to right wheel of the wheelset
2	index related to left wheel of the wheelset
20	index related to 1/20 rail inclination
40	index related to 1/20 rail inclination